# A new nano $CoFe_2$ alloy precursor for cobalt ferrite production via sonoreduction process

**Maya Mohan, Vimlesh Chandra and S. Sundar Manoharan***

Materials Chemistry Laboratory, Department of Chemistry, Indian Institute of Technology, Kanpur 208 016, India

**We have isolated a stable nano bcc-$CoFe_2$ alloy using a combi-sonoreduction process under basic conditions, serving as a potential precursor for $CoFe_2O_4$ production. X-ray and transmission electron microscopy (TEM) confirms the formation of a bcc phase $CoFe_2$ alloy with particle size <10 nm, having spherical morphology. The thermo gravimetric analysis (TGA) confirms the alloy composition, showing a weight gain between 200 and 500°C, leading to a fully oxidized $CoFe_2O_4$. A significant increase in the saturation magnetization ($M_s$ = 230 emu/g) for the nano $CoFe_2$ alloy is observed compared to the theoretical bulk value (200 emu/g) at 300 K.**

**Keywords:** $CoFe_2$ alloy, infrared spectroscopy, saturation magnetization, sonoreduction.

THE equilibrium phase diagram of the Fe–Co alloy suggests that the $Fe_{2/3}Co_{1/3}$ phase exits in $\alpha$-Fe bcc phase. Conventional metallurgical ball milling technique is the most desired route to stabilize such alloy phases. However, use of such alloys as precursors to spinel ferrites is limited due to experimental severities. Wet chemical routes[1] employing hydroxides, nitrates, carbonates, acetates, citrates and hydrazine carboxylate precursors have provided the needed support to synthesize ferrite in bulk quantities, especially for use in magnetic fluids, transformer cores, spintronics, high-frequency applications and in guided drug delivery[2–5]. The use of nanoparticles and nanomaterials in magnetic recording application has led to the reinvestigation of industrially important ferrites in nano dimension[5]. Large-scale application of ferrites of nanometre size and the tailoring of magnetic properties have prompted the development of several widely used methods, including sonochemical reaction[6], sol–gel technique[7], precipitation[8], micro-emulsion procedure[9], mechanical alloying[10], and reverse micelle technique[11] for the preparation of stoichiometric and chemically pure spinel ferrite nanoparticles. Among the many approaches to prepare ferrite particles, a recent route reported by Liu *et al.*[12] involves decomposition of layered double hydroxide precursor. Mooney *et al.*[13] have employed alkalide reduction route employing K–Na alloy and crown ether to prepare cobalt ferrites. Recently, Doh *et al.*[14] reported synthesis of ferrites by coprecipitation process with ultrasound irradiation for 6 h and heated the precipitate at 120°C for 12 h to obtain ferrite powder.

In our attempt to prepare scalable quantities of industrially important ferrites, we incidentally observed that, by a judicious choice of the preparation protocol, one could obtain with ease, either a stable $CoFe_2$ alloy as precursor for $CoFe_2O_4$ or the oxide directly in a single pot reaction. The combi approach that we adopted involves sonoreduction route under alkaline condition. The novelty of this combi approach lies in the use of two techniques, sequentially and simultaneously as a one-pot reaction. The first step involves reduction of metal salts to corresponding metals in nano size, employing $N_2H_4 \cdot H_2O$ as a reducing agent. On reducing the metal salts to metal powders, $N_2H_4 \cdot H_2O$ gets oxidized to $N_2$ and $H_2O$ as by-products, which leaves the metal alloy or oxide products free from any impurity. Upon *in situ* formation of nano metals, chemical effects of ultrasound provide the alloying effect leading to either a stable alloy precursor, $CoFe_2$, if the sonication is carried out in Ar–$H_2$ atmosphere, or finely divided $CoFe_2O_4$ nanoparticles if the reaction vessel is flushed with oxygen atmosphere. Our results indicate a convenient route to the alloy and to oxidize the metal alloys to the desired size and shape using the sonoreduction route.

Analytical grade (Fluka) metal halides were weighed in stoichiometric amounts, dissolved in double distilled water and purged with $N_2$ atmosphere. To this solution, 10 ml of 80 : 20 proportion of $N_2H_4 \cdot H_2O$ in 0.1 M NaOH solution was added. The solution mixture was sonicated (using Misonix, Model XL2020 with Ti Horn, 20 kHz, 100 W/sq. cm) for 30 min in Ar/$H_2$ atmosphere. The resulting black powder was washed repeatedly with distilled water, acetone and dried in vacuum for 48 h. The dried sample was used for thermo gravimetry, powder X-ray and TEM studies. Preparation of $CoFe_2O_4$ was achieved as described above, with the only modification being sonication of the solution in $O_2$ atmosphere instead of Ar/$H_2$. Figure 1 *a* shows the TEM image of the as-prepared alloy, having spherical morphology with an average size of ~10 nm. In Figure 1 *b*, the high-resolution transmission (HRTEM) image shows $CoFe_2$ lattice fringes having a *d*-spacing of 0.203 nm. This value gives an estimated lattice parameter of $a$ = 2.870 Å, which is in good agreement with the experimental value (2.867 Å) calculated from the powder X-ray diffraction (XRD) data. Phase identification was performed by XRD using $CuK_\alpha$ radiation ($\lambda$ = 0.154 nm). The X-ray pattern (Figure 2 *a*) shows that the $CoFe_2$ alloy crystallizes in the $\alpha$-Fe phase, with a lattice constant $a$ = 2.867 (±0.003) Å, which corresponds to the bcc phase of bulk iron. The crystallite size of the as-prepared sample was calculated from the X-ray line broadening using Debye–Scherrer equation: $D = 0.9\lambda/\beta \cos\theta$, where $\beta$ is the full width at half maximum (in radians) of the hkl peak. The average crystallite size was found to be 10 nm, which is in good agreement

*For correspondence. (e-mail: ssundar@iitk.ac.in)

with the TEM observation (Figure 1 *b*). Thermo gravimetric analysis of the stable $CoFe_2$ alloy powder measured in a stream of air, shows a steady increase in weight up to 450°C (Figure 2 *b*). The weight gain was about 22% against a theoretical value of 27%, suggesting that a partial surface oxidation of $CoFe_2$ could be possible during the synthesis, although not evident from the powder X-ray pattern. The alloy is converted to $CoFe_2O_4$ between 200 and 500°C (Figure 2 *a*). The DSC curve for the as-prepared alloy in air is shown in Figure 2 *b* (inset). This curve shows a weak exothermic peak at 260°C, which could be associated with the phase transformation of bcc to bct (since we do not see any weight loss/gain in the TGA curve). The exothermic peak around 400°C is associated with the oxidation of the alloy, suggesting that the alloy undergoes an autocatalytic conversion to the $CoFe_2O_4$ phase due to high reactivity owing to nanosize morphology. Further, Figure 2 *b* presents the infrared spectra for the $CoFe_2O_4$ sample, which shows characteristic high frequency IR bands corresponding to intrinsic vibration of the tetrahedral sites.

The transmission electron micrograph (Figure 3 *a*) presents the morphology of the as-prepared $CoFe_2O_4$ powder, which shows weakly agglomerated spherical particles with uniform size (~20 nm). The scanning electron micrograph (Figure 3 *b*) provides an idea of the agglomerated clusters of cobalt ferrite powder with uniform size and shape that can be realized by oxidizing the $CoFe_2$ alloy powder sonochemically. In Figure 4, we show the progressive evolution of magnetization, starting from the $CoFe_2$ alloy to the corresponding oxide. The magnetic hysteresis loop measurements done at 300, 200 and 100 K show characteristic ferromagnetic behaviour, with the

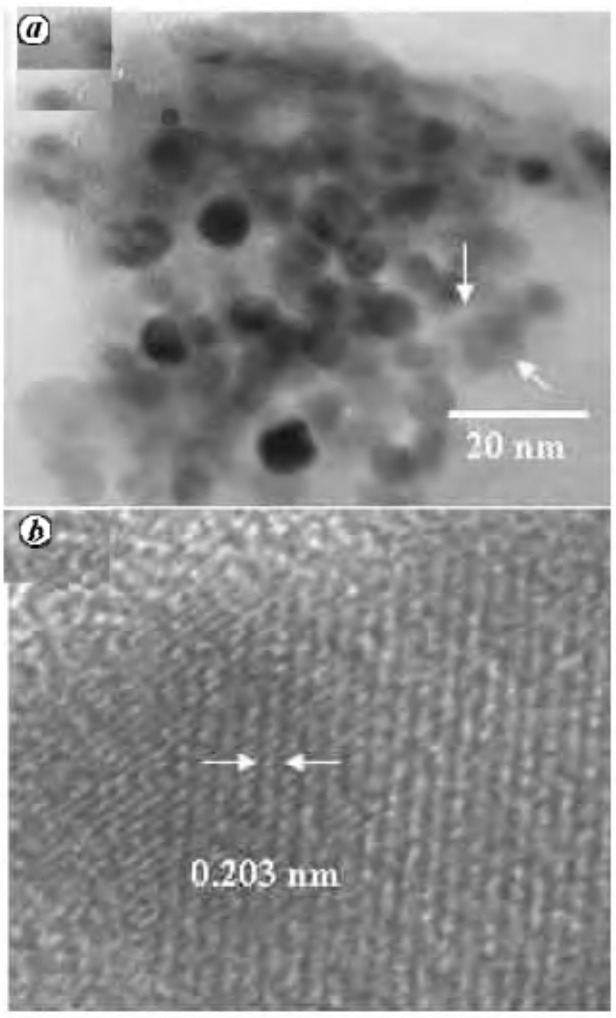


**Figure 1.** ***a***, TEM image showing morphology of as-prepared $CoFe_2$ alloy. Moiré fringes are evident in these nano alloy particles, which are free from agglomeration without any surfactant effect. ***b***, HRTEM image showing $CoFe_2$ lattice fringes with *d*-spacing of 0.203 nm.

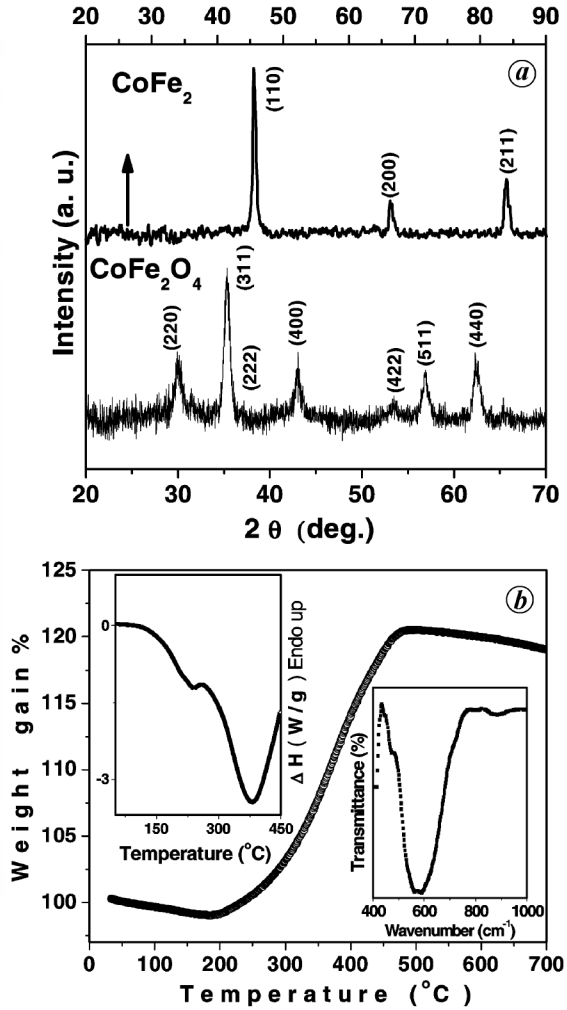


**Figure 2.** ***a***, X-ray diffraction pattern of as-prepared $CoFe_2$ alloy is isomorphous with the $\alpha$-Fe system. Miller indices for each reflection are shown in parenthesis. $CoFe_2$ is further converted to $CoFe_2O_4$, which shows the spinel phase. Note the ease with which crystalline alloys can be isolated via the sonoreduction route, which otherwise yields nano amorphous alloys employing conventional sonochemical methods. ***b***, TG–DSC plot for the $CoFe_2$ alloy composition. The 22% weight gain (DSC peak at 400°C) corresponds to $CoFe_2 \rightarrow CoFe_2O_4$ conversion under $O_2$ atmosphere. Infrared spectra further confirm $CoFe_2O_4$ formation.

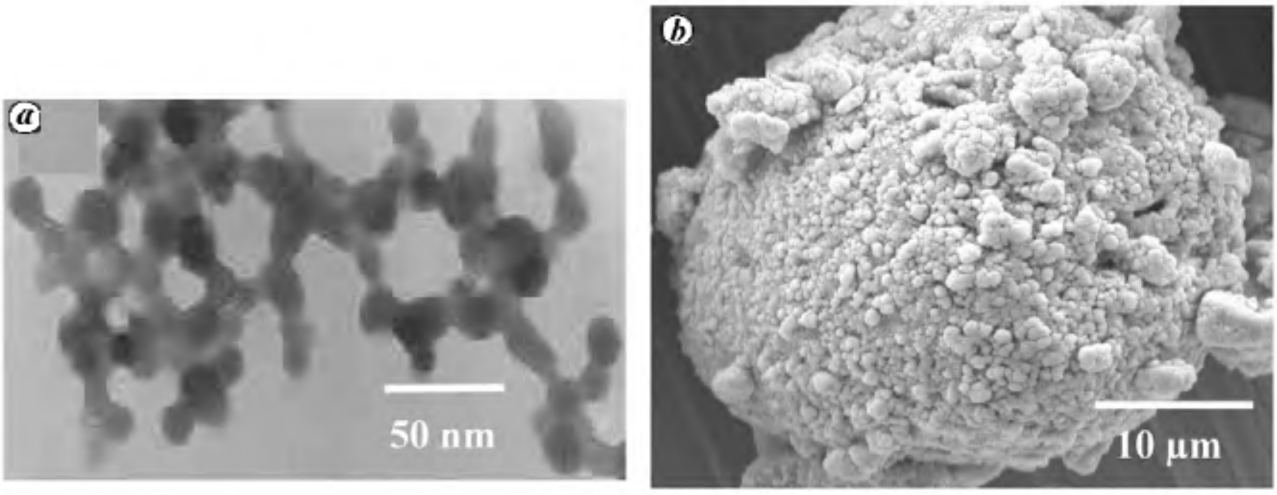


**Figure 3.** ***a***, Transmission electron micrograph of as-prepared $CoFe_2O_4$ showing weakly agglomerated, nearly spherical particles of 20 nm size. ***b***, Scanning electron micrograph of as-prepared nano $CoFe_2O_4$ powders showing agglomerates of mono-sized particles.

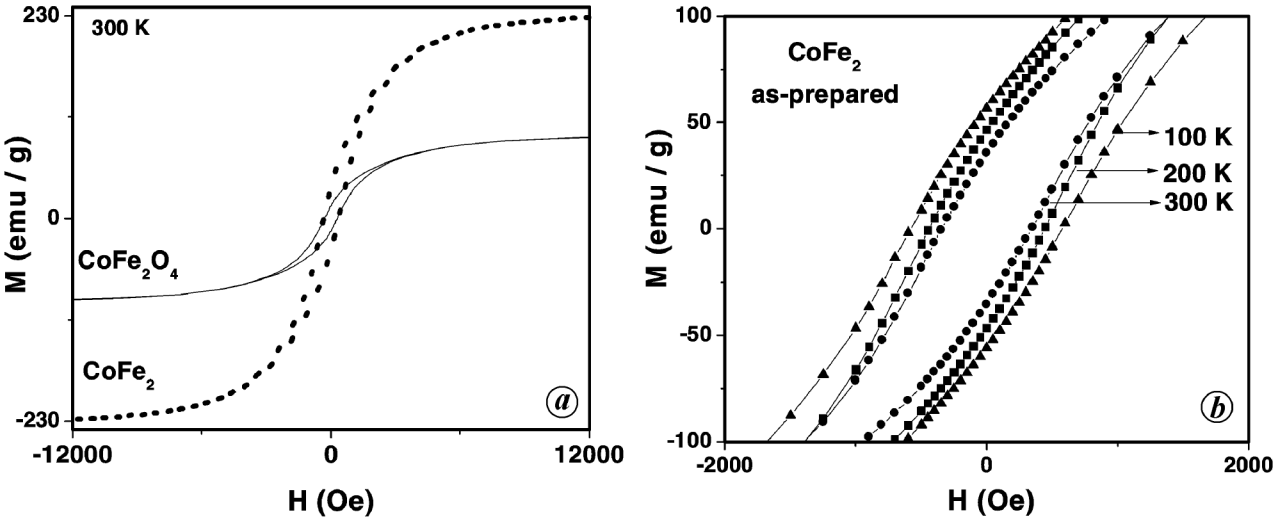


**Figure 4.** ***a***, Hysteresis loops of as-prepared $CoFe_2$ alloy and $CoFe_2O_4$ recorded at 300 K showing the relative room temperature magnetization of the alloy and the ferrite. ***b***, Hysteresis loops of as-prepared $CoFe_2$ alloy at 100, 200 and 300 K. Note the increase in coercivity as we cool the sample from 300 K.

coercivity decreasing with increasing temperature. Significantly, the Curie temperature of the alloy is >>300 K. The saturation magnetization of the alloy at room temperature was 230 emu/g (7.018 $\mu_B$), which is close to the theoretical value of 200 emu/g (6.16 $\mu_B$). On complete oxidation of $CoFe_2$ to $CoFe_2O_4$, the sample shows a typical soft magnetic behaviour.

In summary, we have studied the structure and magnetic properties of sonochemically prepared nano bcc-$CoFe_2$ alloy using the sonoreduction principle. The sonoreduction process appears to be a convenient route to prepare X-ray crystalline nano-alloys. Although several wet chemical routes offer low-temperature processing pathways against the conventional solid-state route, the use of alloy precursor to synthesize ferrites at temperatures <400°C holds promise for possible scale-up processes. The main incentive comes from keeping both the alloy and the oxides free from other by-product impurities.

1. Patil, K. C., Manoharan, S. S. and Gajapathy, D., *Preparation of High Density Ferrites* (ed. Cheremisinoff), Marcel Dekker, New York, 1989, vol. 1, pp. 469–493.
2. Berry, C. C. and Curtis, A. S. G., Fictionalization of magnetic nanoparticles for application in biomedicine. *J. Phys. D: Appl. Phys.*, 2003, **36**, R198–R206.
3. Luders, U. *et al.*, $NiFe_2O_4$: A versatile spinel material brings new opportunities for spintronics. *Adv. Mater.*, 2006, **18**, 1733–1736.
4. Wang, Z. L., Liu, Y. and Zhang, Z., *Handbook of Nanophase and Nanostructured Materials*, Kluwer/Plenum Publishers, New York, 2002, vol. 3.

5. Weller, D. *et al.*, High $K_u$ materials approach to 100 Gbits/in$^2$. *IEEE Trans. Magn.*, 2000, **36**, 10–15.
6. Shafi, K. V. P. M. and Gedanken, A., Sonochemical preparation and size-dependent properties of nanostructured $CoFe_2O_4$ particles. *Chem. Mater.*, 1998, **10**, 3445–3450.
7. Willey, R. J., Oliver, S. A., Oliveri, G. and Busca, G., Chemistry and structure of mixed magnesium ferric oxide aerogels. *J. Mater. Res.*, 1993, **8**, 1418–1427.
8. Kulkarni, R. G. and Joshi, H. H., Comparison of magnetic properties of $MgFe_2O_4$ prepared by wet-chemical and ceramic methods. *J. Solid State Chem.*, 1986, **64**, 141–147.
9. Liu, C., Rondinone, A. J. and Zhang, Z., Synthesis of magnetic spinel ferrite $CoFe_2O_4$ nanoparticles from ferric salt and characterization of the size-dependent superparamagnetic properties. *J. Pure Appl. Chem.*, 2000, **72**, 37–45.
10. Chinnasamy, C. N. *et al.*, Mixed spinel structure in nanocrystalline $NiFe_2O_4$. *Phys. Rev. B*, 2001, **63**, 184108–184114.
11. Kale, A., Gubbala, S. and Misra, R. D. K., Magnetic behaviour of nanocrystalline nickel ferrite synthesized by the reverse micelle technique. *J. Magn. Magn. Mater.*, 2004, **277**, 350–358.
12. Liu, J., Li, F., Evans D. G. and Duan, X., Stoichiometric synthesis of a pure ferrite from a tailored layered double hydroxide (hydrotalcite-like) precursor. *Chem. Commun.*, 2003, 542–543.
13. Mooney, K. E., Nelson, J. A. and Wagner, M. J., Superparamagnetic cobalt ferrite nanocrystals synthesized by alkalide reduction. *Chem. Mater.*, 2004, **16**, 3155–3166.
14. Doh, S. G., Kim, E. B., Lee B. H. and Oh, J. H., Characteristics and synthesis of Cu–Ni ferrite nanopowders by coprecipitation method with ultrasound irradiation. *J. Magn. Magn. Mater.*, 2004, **272**, 2238–2240.

ACKNOWLEDGEMENT. We thank the Council of Scientific and Industrial Research, New Delhi for financial support.

Received 3 September 2007; revised accepted 19 December 2007

# The expanding Indian desert: Assessment through weighted epochal trend ensemble

**P. Goswami* and K. V. Ramesh**

CSIR Centre for Mathematical Modelling and Computer Simulation, Wind Tunnel Road, Bangalore 560 037, India

**One of the biggest challenges in climate research is to arrive at reliable future projections. However, while there now exists a firm scientific basis and procedure for climate forecasts, numerical climate models still suffer from large uncertainties. Observed local trends do reflect the combined effect of both anthropogenic forcings and natural variability over a location; however, projections based on a linear trend may have considerable error as the trends are generally significantly nonlinear owing to low-frequency natural variability and resultant changes (second derivatives) in the trends. Here we adopt a weighted epochal trend ensemble approach to assess the stability of the Indian desert with increased reliability. Ensemble techniques have generally helped to reduce uncertainties in forecasts and the weighted epochal trend ensemble proposed here takes into account the inherent nonlinearity in the trend by considering a piece (epoch)-wise linear trend and its weighted contributions to construct more reliable future projections of local climate change. We first show that epochal trend ensemble provides better estimates of future projections by comparing observed rainfall over India during 1990–2003 with rainfall projected from a simple linear trend and an epochal trend ensemble. We then compute projections of desert area over India based on annual rainfall and show that the Thar Desert in western India is expanding in an eastward as well as northeast direction. Both the simple linear trend and the epochal trend ensemble projections indicate significant increase in the desert area over India over the next 100 years; however, there are also significant differences between the two projections. The results of the validation are used to choose the more reliable projection, which shows a sharp increase in the size of the Indian desert in the next hundred years.**

**Keywords:** Climate change, future projection, Indian desert, simple linear trend, weighted epochal trend ensemble.

ONE of the serious and possible consequences of global warming and climate change is the shift in precipitation patterns leading to aridity or hyper-aridity over certain locations, especially over semi-arid regions that suffer from persistently negative trends in precipitation. Although global warming is generally associated with a wetter climate owing to a general increase in tropospheric moisture[1], local effects of climate change could be reduced rainfall. For example, as shown in Figure 1, linear trends in both rainfall and surface temperature show significant spatial variability with negative trend over many places, even though the large-scale area-averaged rainfall may be stable. Although modern-day climate models based on atmospheric general circulation or ocean–atmosphere coupled models provide quantitative assessment of future climates for a given scenario (like $CO_2$ doubling), these forecasts are necessarily not unique and suffer from significant uncertainties due to intra-model (resolution, parameterization, etc.) and inter-model dispersions in the simulations[2–6]. In contrast, observed trends reflect the collective effects of various factors and allow reliable estimation of future projections. However, projections based on linear trends, even with statistical significance, are not always reliable as the linear trends often possess significant second derivatives (their own dynamics). The epochal (10 yrs) variability of linear trends in area-averaged annual rainfall is shown in Table 1 for three areas. The trends in large-scale area averages show significant epochal variability. With

*For correspondence. (e-mail: goswami@cmmacs.ernet.in)